# Supplementary Figure legends

**Supp Figure 1. Humoral response to COVID-19 infection in infants, related to Figure 1**

A) Summary of the conducted assays. B,C) Kinetics of developing binding (B) and neutralizing (C) antibody response in infants with COVID-19. D,E) Comparison of binding (D, Non-Omi n = 13, Omi n = 18, Conv n = 30) and neutralizing (E, Non-O n = 13, Omi n = 18) titers between different variants in infants. E) Kinetics of specific autoantibodies which increased during or after COVID-19. Initial statistical comparisons were conducted in a paired fashion with the Wilcoxon signed rank test (Pre vs. Conv, n = 27) and Benjamini-Hochberg correction. Validation tests (M-ctrl vs. Conv) were conducted using Wilcoxon rank sum test (conv n = 30, m-ctrl n = 27).

**Supp Figure 2. Prevalence of autoantibodies in infants with COVID-19, related to Figure 1**

Heatmap depicting plasma IgG antibodies against the indicated autoantigens and cytokines and chemokines. Prototypes (n=15), adult controls (n=10), adults with acute COVID-19 infection (n=15), infant controls who have not had COVID-19 (n=27), and longitudinal samples from infants who had COVID-19 (pre-infection (n=27), acute infection (n=19), acute omicron infection (n=18), and convalescent samples (n=30)) are shown. Prototypes are positive control samples from patients with known autoimmune disorders. Colors indicate autoantibodies with MFI >5 SD (red) or <5 SD (black) above average for healthy infants. MFIs <3000 were excluded.

**Supp Figure 3. Memory B and T cell response, related to Figure 2**

A) Gating strategy used for SARS-CoV-2 spike specific IgG+ memory B cell staining and single-cell sorting. Gating was on singlets that were CD20+ and CD3- CD14- IgM- IgD- CD27low/+ IgG+. Sorted cells were Wuhan spike-AlexaFluor 488+ and/or Omicron spike-BV421+. B) The percentage of SARS-CoV-2 spike-specific IgG+ memory B cells in healthy, acute, and convalescent infant individuals. The sample number for each group is indicated in brackets. C) As in (B), the percentage of SARS-CoV-2 spike-specific IgG+ memory B cells in adult individuals with mild, severe, and ICU symptoms and in adult convalescent individuals. The sample number for each group is indicated in brackets. D-F) T cells were stimulated with overlapping peptides against WT (D-F) and Omicron (F) variants. Cytokine production was determined via flow cytometry. D) Box plot showing the fraction of responding T cells at different infection stages. E) Box plot showing the fraction of multifunctional T cells at different infection stages. F) Comparison of the multifunctional T cell response after stimulation with WT and Omicron (Om) peptides. Statistical comparisons were conducted with Wilcoxon rank sum test.

Solid line indicates median healthy response; dashed line indicates 3x median healthy response.

**Supp Figure 4. Cytokine response to COVID-19 infection in infants, related to Figure 3**

A) Comparison of key inflammatory mediators during COVID-19 infection in infants and adults, stratified by severity. Infant infection was overall mild or asymptomatic. B,C) Comparison of plasma IFNα2 levels between Non-Omicron (Non-O, n = 19) and Omicron (Omi, n = 22) infected infants (B), and infants (n = 41) and adults (n = 15) (C). Statistical comparisons were conducted with the unpaired t-test (A) and Wilcoxon rank sum test (B,C).

**Supp Figure 5. Cellular immune response to COVID-19 infection, related to Figure 4**

A) Heatmap showing the expression of CyTOF markers in all manually gated subsets. B) Correlation analysis between the frequency of indicated cell types (y-axis) and plasma IFNα2 levels (x-axis). C) Heatmap showing the expression levels of significantly changed markers in healthy and infected samples. Colors indicate the infection stage. D) Boxplots showing the frequency of pDCs as a proportion of total CD45+ cells (left) and the expression of pS6 in pDCs for different infection stages. E) Boxplots showing HLA-DR expression on mDCs for different infection stages. Correlation analyses were conducted using Spearman correlation.

**Supp Figure 6. Single-cell multi-omics analysis of immunity to COVID-19 infection in infants, related to Figure 5**

A) Full ring plot from Figure 5c. Pairwise comparison of genes from healthy (n = 16) and COVID-19–infected infants at different times during acute infection (D0-5: n = 5, D5-10: n=7, D10+: n=6) was conducted for each cluster. DEGs were analyzed for the enrichment of BTMs. Ring plot shows an abridged representation of enriched pathways in each cluster. Size indicates the number of samples with enrichment; colors indicate the normalized enrichment score. B) UMAP representation of the integrated analysis of monocyte clusters from this study and from adult COVID-19 patients [21] and adult subjects immunized with the COVID-19 vaccine [30]. Colors indicate the study origin of cells (top), the cell cluster (middle), and the expression of ISGs (bottom). C) DEGs determined between infant C14.1 and adult COVID-19-infection C11 monocyte clusters are plotted and ranked by fold change. C) DEGs determined between infant C14.1 and adult vaccination C8 monocyte clusters are plotted and ranked by fold change. D) Correlation analysis between plasma IFNα2 levels and average ISG levels in each cell type. E)

Heatmap showing expression of NK cell activation genes enriched in NK cells in Figure 5c (green box).

**Supp Figure 7. Single-cell epigenomic analysis of immunity to COVID-19 infection in infants, related to Figure 6**

A) Pairwise comparison of TF motif accessibility between convalescent and pre or matched-ctrl samples was conducted for each cluster. Color indicates difference in TF accessibility; non-significant changes (FDR>=0.0001 or changed in less than two subjects) are grey. Size indicates the number of samples with significant change. (pre: n = 9, matched-ctrl: n = 7, Conv: n = 9) B) Box plot showing sample-level accessibility of selected TFs from (A) in CD14+ monocytes. C) Gene tracks showing chromatin accessibility at indicated time points in CD16+ monocytes.

**A**

| Assay | Sample type | Infants | | | | | Adults | | | |
|---|---|---|---|---|---|---|---|---|---|---|
| | | pre | acute | | conv | ctrl | acute | conv | ctrl | total |
| | | | non-omicron | omicron | | | non-omicron | | | |
| S-Specific B cells | pbmc | 12 | 12 | 3 | 21 | 10 | 17 | 2 | | 77 |
| Antigen-specific T cells | pbmc | 12 | 12 | 3 | 21 | 10 | 16 | 2 | | 76 |
| CyTOF | pbmc | 14 | 19 | 14 | 14 | 14 | | | | 75 |
| scMultiomics | pbmc | 9 | 10 | 8 | 9 | 7 | | | | 46 |
| MSD antibody binding titer | plasma | 27 | 19 | 18 | 30 | 5 | 15 | 10 | 4 | 128 |
| Olink inflammation panel | plasma | 27 | 19 | 18 | 30 | 27 | 15 | | 10 | 146 |
| MSD IFNa2 | plasma | 27 | 19 | 22 | 30 | 27 | 15 | | 10 | 150 |
| Neutralizing titers | serum | 27 | 19 | 18 | 30 | | 16 | | | 110 |
| Neutralizing titers -Omicron subt. | serum | 27 | 19 | 18 | 30 | | | | | 94 |
| Auto-antibodies | plasma | 27 | 19 | 18 | 30 | 27 | 15 | | 10 | 146 |
| bulkRNA-seq | tempus | 27 | 19 | 18 | | 26 | | | | 90 |

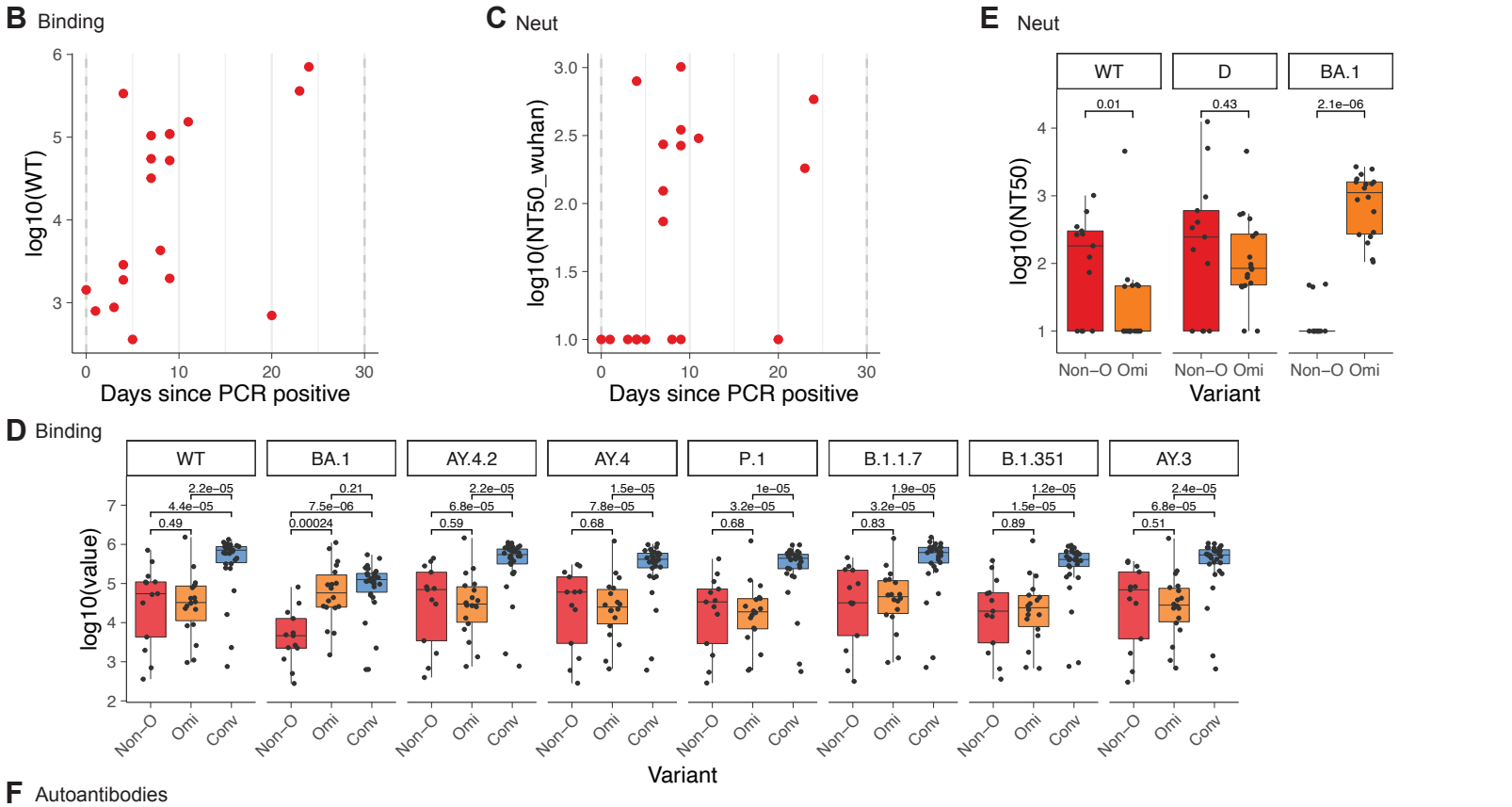


**F** Autoantibodies

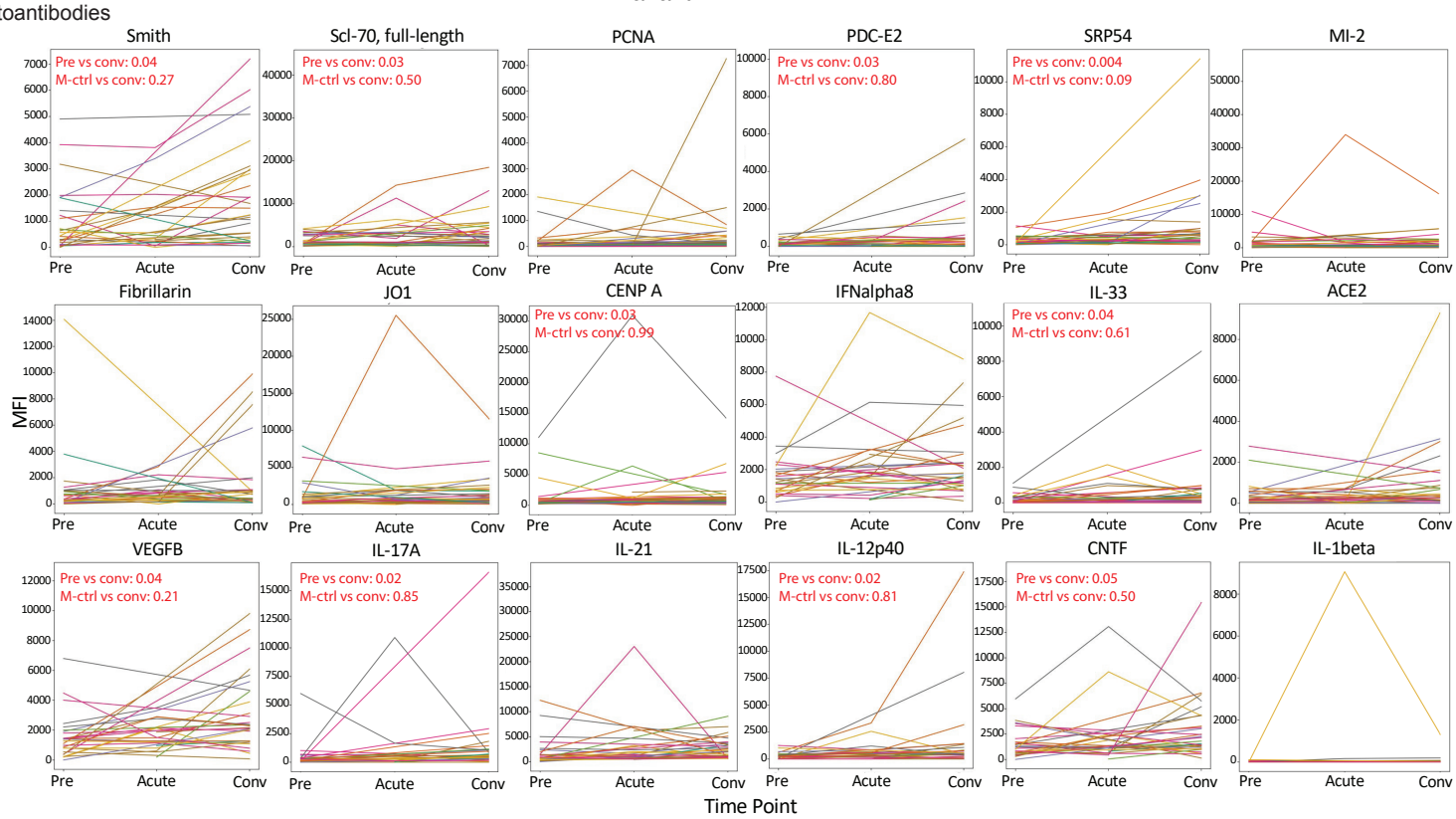

Supp Figure 2

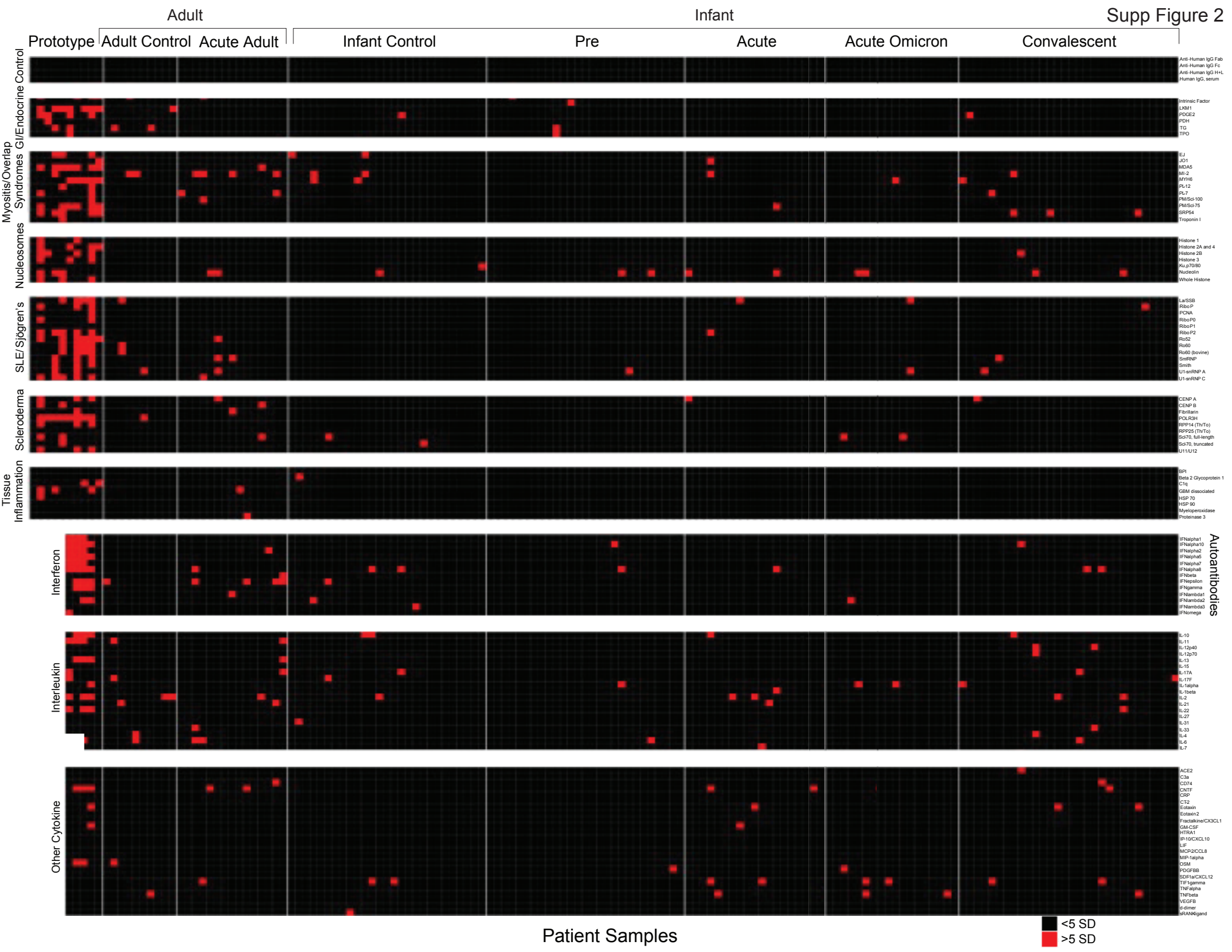

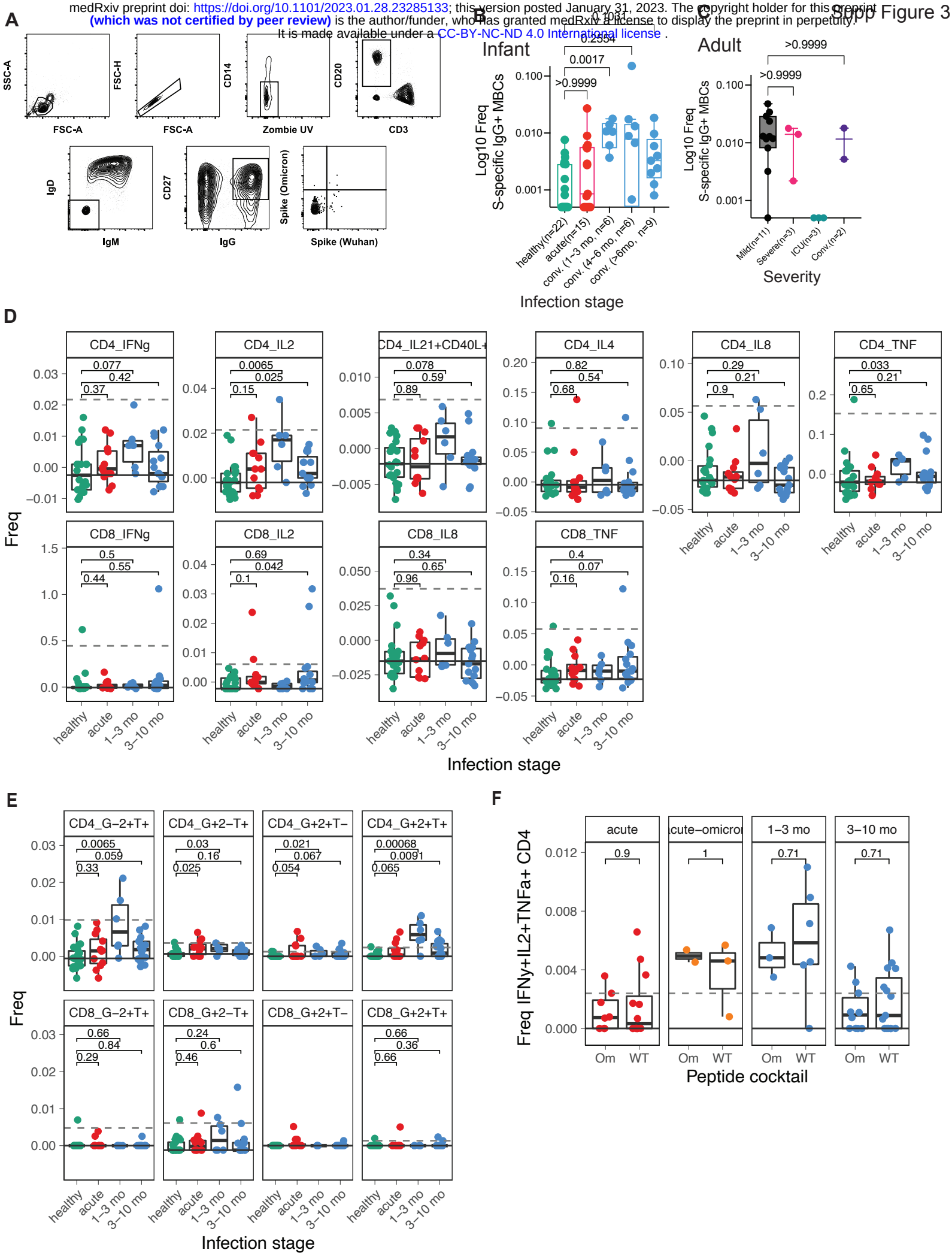

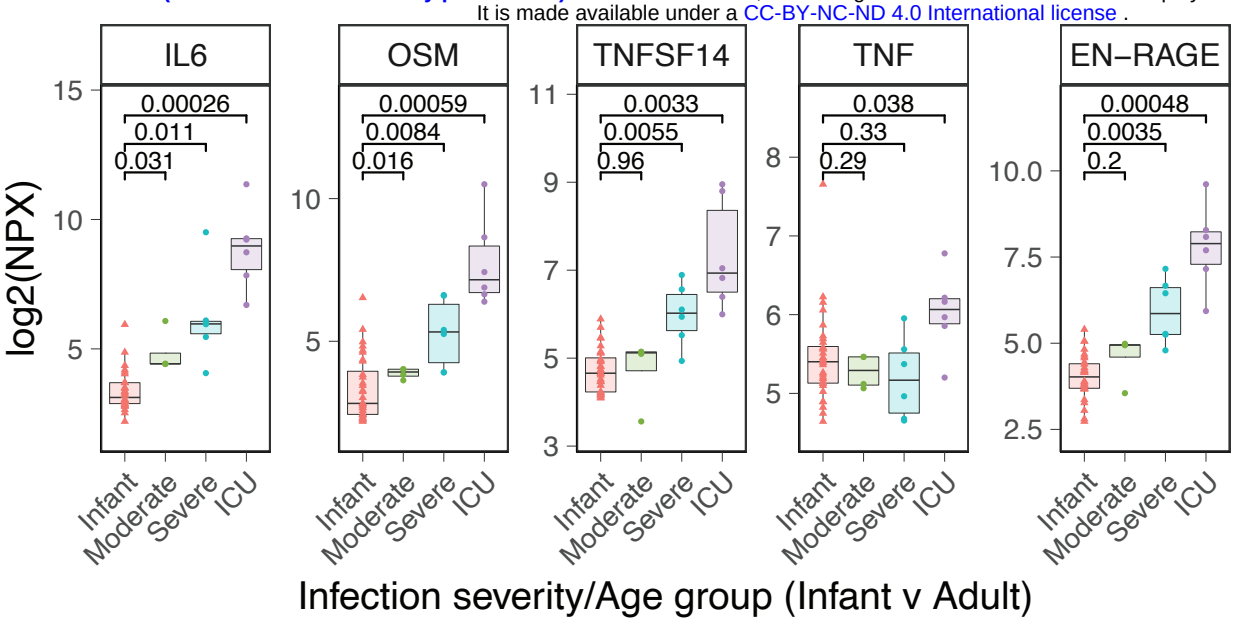


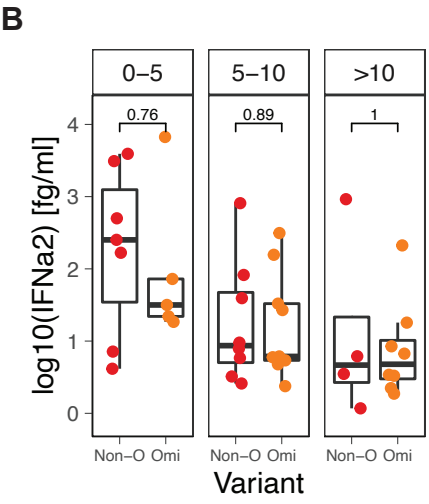


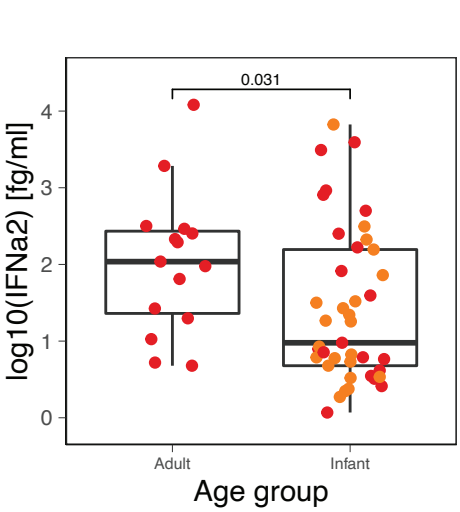

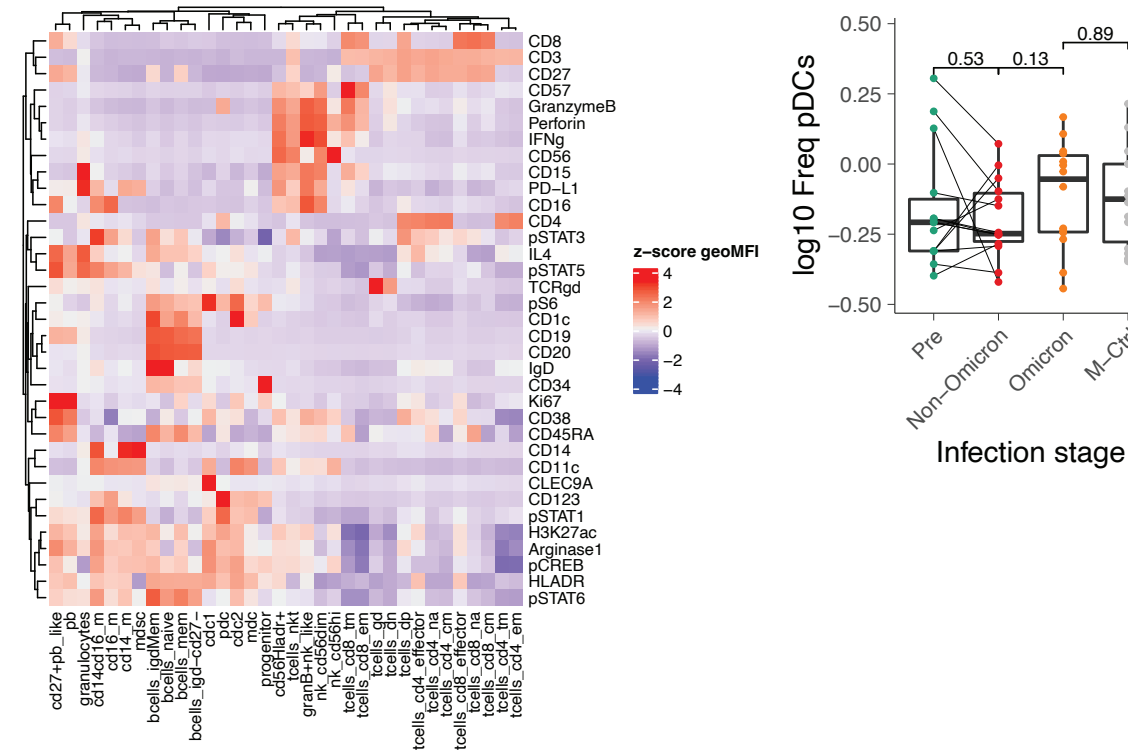


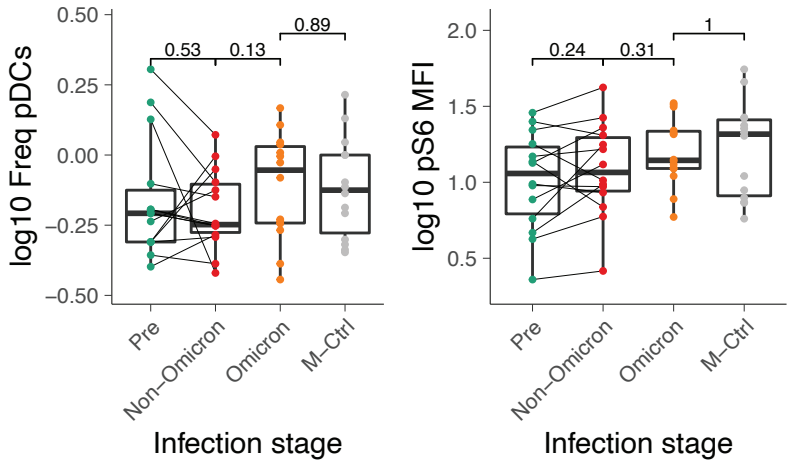


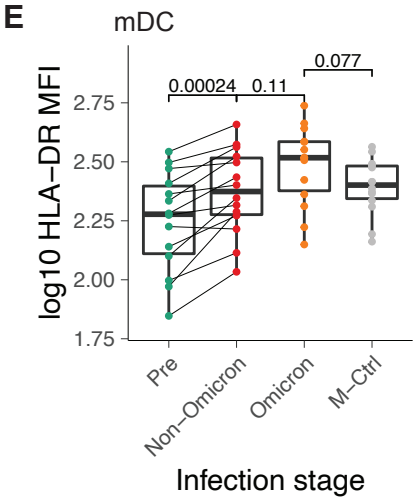


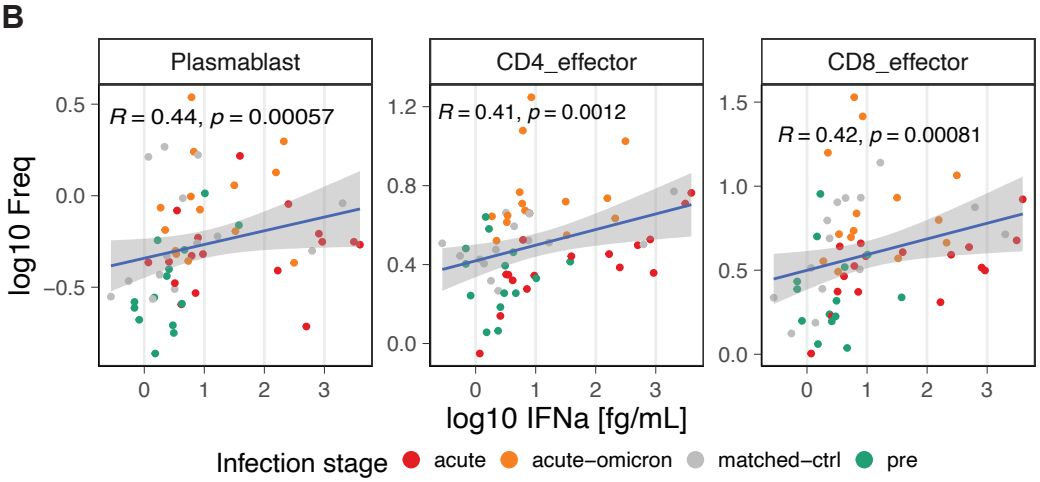


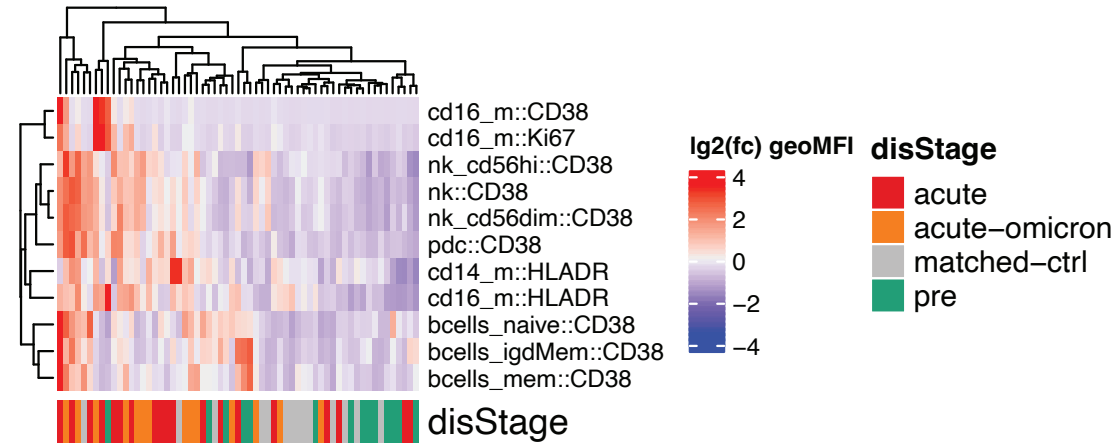

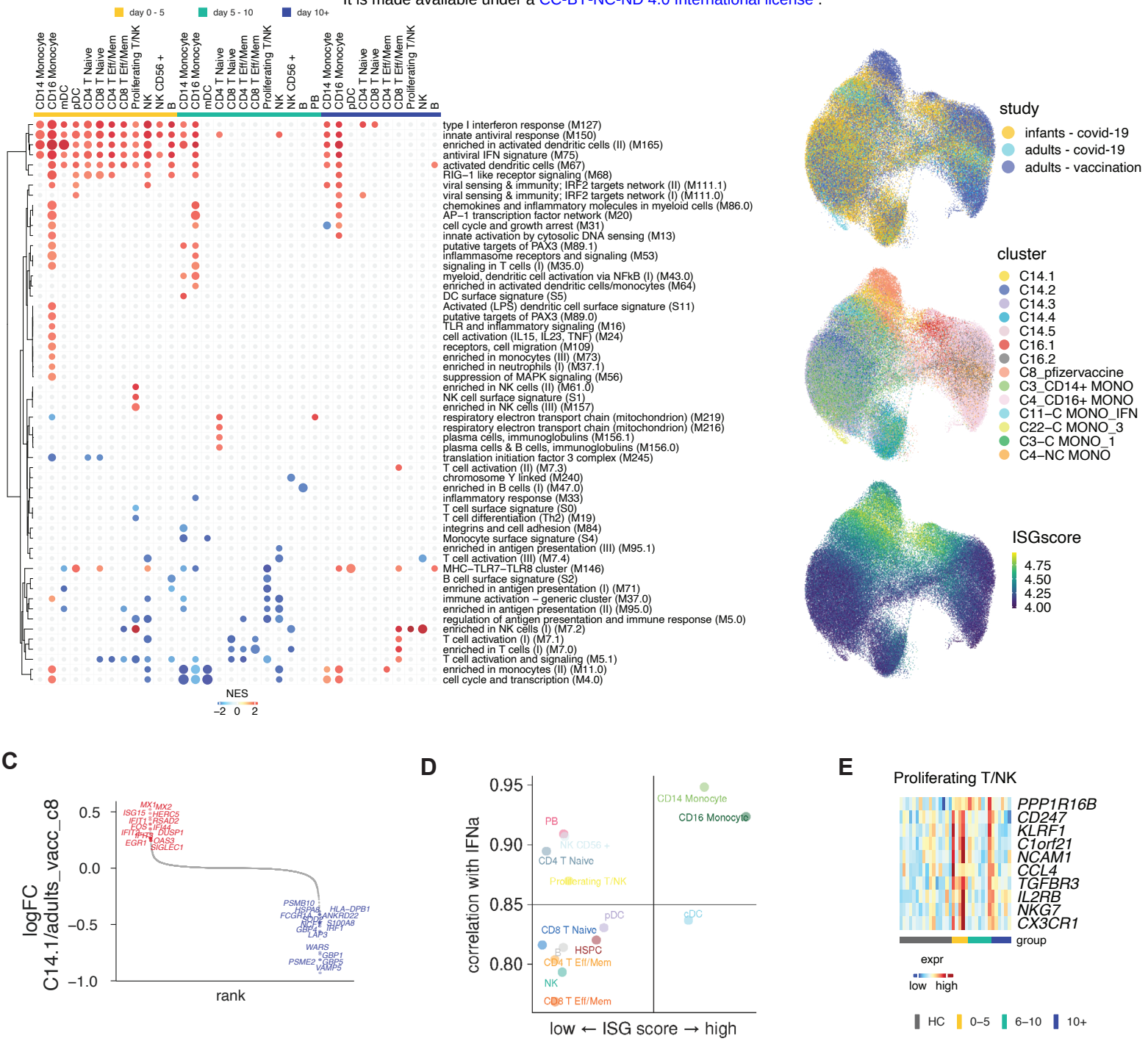

**A**

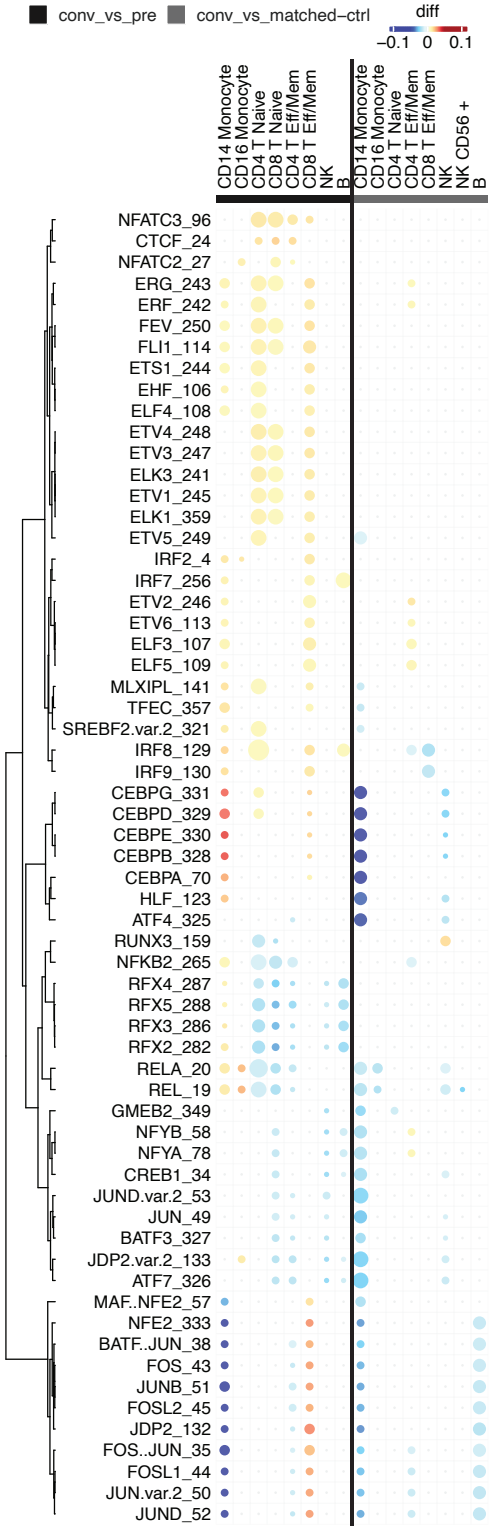


**B**

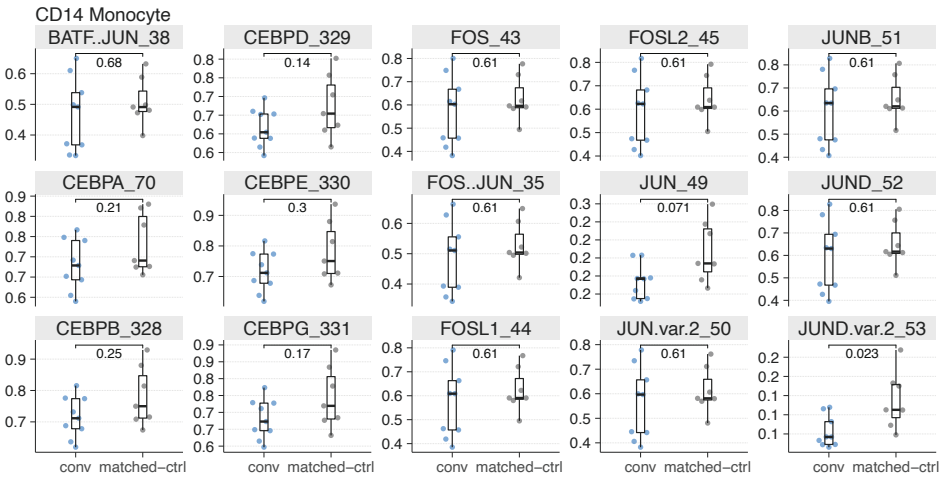


**C**